PNL-SA--21261

DE92 041342

INTERACTIONS BETWEEN MANGANESE OXIDES AND MULTIPLE-RINGED AROMATIC COMPOUNDS

G. Whelan
R. C. Sims*

August 1992

Presented at the ISSS Working Group MO
August 10-16, 1992
Edmonton, Canada

Prepared for
the U.S. Department of Energy
under Contract DE-AC06-76RLO 1830

Pacific Northwest Laboratory
Richland, Washington

*Utah State University, Logan, Utah

INTERACTIONS BETWEEN MANGANESE OXIDES AND MULTIPLE-RINGED AROMATIC COMPOUNDS

G. Whelan** and R. C. Sims

Department of Civil and Environmental Engineering
Utah Water Research Laboratory, UMC-8200
Utah State University
Logan, Utah 84322-8200

TABLE OF CONTENTS

**To whom correspondence may be addressed. Currently located at Battelle, Pacific Northwest Laboratories, P.O. Box 999, K6-77, Richland, Washington 99352.

I. INTRODUCTION

Biochemical and chemical biotic/abiotic oxidation, immobilization, and detoxification of recalcitrant organics, including polynuclear aromatic hydrocarbons (PAHs), may serve as a basis for in situ and at-grade treatment of certain organic wastes. Current research has focused on enzymatic-catalyzed oxidation of pesticides and single-ringed aromatics.[1-4] For example, Bollag and Myers[5] concluded that biotic polymerization of xenobiotics in a humification process is possible because many of the degradation products of pesticides result in the formation of reactive intermediates with structures and/or functional groups similar to those found in natural humus material. Humus materials are natural organic substances that are common in the environment and are involved in nonstop polymerization process with organic molecules.[6]

Recently, scientists have noted that abiotic-catalyzed polymerization may also represent an important aspect of humification.[7-11] Manganese-bearing silicates have demonstrated catalytic effects in enhancing the polymerization of polyphenols (e.g., hydroquinone).[11] Research is beginning to focus more on how abiotic catalysis affects the oxidation process (e.g., humification/polymerization) of organics and multiple-ringed aromatics.[12-16]

Research has demonstrated that aromatic compounds containing diol and dione functional groups tend to be susceptible to abiotic-catalyzed oxidation and also suggested that an increase in reactivity among diol compounds can be attributed to the ability of these compounds to form a corresponding quinone through a resonance-stabilized semiquinone radical.[17-18] Figure 1 presents a proposed relationship between naphthalenediol, semiquinone radical, naphthoquinone, semiquinone radical anion, and a semiquinone dianion.[19-22]

The objective of this research was to investigate the potential relationship between metallic oxides and PAH compounds through the reductive-dissolution process. Because of its oxidation-reduction (redox) potential, manganese oxides were used to oxidize the following five multiple-ringed aromatic compounds containing diol and dione functional groups under oxic conditions: 1,4-, 1,3-, and 2,3-naphthalenediol [$C_{10}H_6(OH)_2$]; 1,4-naphthoquinone ($C_{10}H_6O_2$); and 1,4-dihydroxy-9,10-anthracenedione [Quinizarin, $C_{14}H_6O_2(OH)_2$]. Figure 2 presents a schematic of each compound. In many instances, naphthalenediol has been chosen to illustrate relationships between the manganese oxides and organic substrates; any one of the other aromatic constituents could also have been chosen.

II. STOICHIOMETRY OF REDUCTIVE DISSOLUTION AND AUTO-OXIDATION

Whelan and Sims[20,22] and Whelan[21] reviewed stoichiometric relationships between Mn(IV) and 1,4-naphthalenediol [i.e., 1,4-dihydroxynaphthalene, Nap-$(OH)_2$] in an oxic environment. If the reaction is assumed to proceed through an organic free radical, the following reaction describes the reductive dissolution of Mn(IV) and oxidation of naphthalenediol [Nap-$(OH)_2$] to form dissolved Mn(II) and a semiquinone radical ($\cdot$O-Nap-OH) (see Figure 1).

$$Mn^{IV}O_2(s) + 2\ Nap\text{-}(OH)_2 + 2\ H^+ = Mn^{2+} + 2\ (\cdot O\text{-}Nap\text{-}OH) + 2\ H_2O \qquad (1)$$

Stone and Morgan[19] have mechanistically described this reductive-dissolution/oxidation process in four steps, assuming inner-sphere complex formation between Nap-$(OH)_2$ and the oxide surface. Whelan and Sims[20,22] and Whelan[21] expressed these as follows:

1. *Precursor-Complex Formation (Reductant Adsorption)*:

$$\equiv Mn^{IV}(OH)_2 + 2\ Nap\text{-}(OH)_2 \underset{k_{-1}}{\overset{k_1}{\rightleftharpoons}} \equiv Mn^{IV}(O\text{-}Nap\text{-}OH)_2 + 2\ H_2O \qquad (2)$$

where the symbol "▪" refers to the oxide surface, and k_1 and k_{-1} are rate constants in the forward and reverse directions, respectively.

2. *Electron Transfer*:

$$\text{▪Mn}^{IV}\text{(O-Nap-OH)}_2 \underset{k_{-2}}{\overset{k_2}{\rightleftharpoons}} \text{▪Mn}^{II}\text{(}\cdot\text{O-Nap-OH)}_2 \qquad (3)$$

where k_2 and k_{-2} are rate constants in the forward and reverse directions, respectively.

3. *Release of Oxidized Organic Product*:

$$\text{▪Mn}^{II}\text{(}\cdot\text{O-Nap-OH)}_2 + H_2O \underset{k_{-3}}{\overset{k_3}{\rightleftharpoons}} \text{▪Mn}^{II}OH_2 + 2\ \text{(}\cdot\text{O-Nap-OH)} \qquad (4)$$

where k_3 and k_{-3} are rate constants in the forward and reverse directions, respectively, and ·O-Nap-OH is a radical. By noting that Mn(II) still resides on the oxide surface, the Mn(II) products of Equation (4) can also be written as follows, because the right- and left-hand sides of Equation (5) are equivalent:

$$\text{▪Mn}^{II}OH_2 \equiv \text{▪Mn}^{IV}O_2\text{-(Mn}^{II}OH_2\text{)} \qquad (5)$$

where "▪$Mn^{IV}O_2$-($Mn^{II}OH_2$)" represents the reduced metal complex on the Mn(IV) surface prior to Mn(II) release. Research has indicated that oxygen promotes oxidative coupling reactions of organics, creating dimers, trimers, and other less soluble, more surface-active oxidation products.[21-28] These oxidative-coupling reactions could account for the removal of radical products that are consumed in the oxidation process.

4. *Release of Reduced Metal Ion*: Stone and Ulrich[29] noted that protons frequently assist in the metal-detachment step of dissolution reactions and that studies have generally found the number of protons involved to be equal to the valence of the detached metal (i.e., 2).[30] They continued to

note that the actual number of protons involved in reductive dissolution is not known with certainty, because the presence of two or more oxidation states on the metal surface may alter the pH dependence of the metal-release step. The release of the reduced metal ion from the surface is expressed as follows:

$$\equiv Mn^{IV}O_2\text{-}(Mn^{II}OH_2) + 2\ H^+ \xrightarrow{k_4} \equiv Mn^{IV}(OH)_2 + Mn^{2+} + H_2O \qquad (6)$$

where k_4 is a rate constant. In experiments to determine the effect of varying amounts of Mn^{2+} on MnO_2 dissolution rates, Stone and Morgan[15] found that initial rates of dissolution with varying amounts of Mn^{2+} in solution had no effect on kinetics. Therefore, one might conclude that Equation (6) is not rate limiting and can be considered to be unidirectional.

As shown schematically (Fig. 3), the auto-oxidation of Mn^{2+} to Mn(IV) can be represented as[31]

$$Mn^{2+} + \tfrac{1}{2}\ O_2 + H_2O = Mn^{IV}O_2(s) + 2\ H^+ \qquad (7)$$

Note that two protons are produced in Equation (7), whereas Equation (1) indicates that two protons are consumed. They also note that the Mn^{2+} concentration decreases with time with an apparent autocatalytic effect. Benefield et al.[32] describe the autocatalytic oxidation of Mn(II) in the following manner:[31,33]

$$d[Mn^{2+}]/dt = - k_5\ [Mn_T]\ [P_{O_2}]\ [OH^-]^2\ [Mn^{2+}]\ [Mn_T - Mn^{2+}] \qquad (8)$$

where k_5 is a rate constant, Mn_T is the total manganese in the system, and $[P_{O_2}]$ is the partial pressure of oxygen. Wehrli[34] noted that thermodynamics indicate that manganese should be present in oxic waters as Mn(IV) oxides; however, experiments and analyses by Diem and Stumm[35] and Wilson,[36] respectively, have indicated that Mn^{2+} is not oxidized by oxygen within several years. Wehrli[34] observed that recent experimental evidence had shown that mineral surfaces provide accelerated

pathways for redox processes such as the oxygenation of metal ions and organic pollutants. He suggested that manganese oxygenation is accelerated by iron oxide particles by a factor of more than 10,000. Whelan and Sims[20,22] and Whelan[21] combined auto-oxidation with these four steps to schematically describe the reductive-dissolution/auto-oxidation process, as illustrated in Figure 3.

Whelan[21] and Whelan and Sims[22] also reviewed potential relationships between naphthalenediol and Mn(III) in an oxic environment, and Mn(IV) and Mn(III) in an anoxic environment. Although the anoxic environment is not discussed herein, the relationship between Mn(III) and naphthalenediol, assuming free-radical complex formation is as follows:

$$Mn^{III}OOH(s) + Nap\text{-}(OH)_2 + 2\ H^+ = Mn^{2+} + \cdot O\text{-}Nap\text{-}OH + 2\ H_2O \qquad (9)$$

For both the oxic and anoxic cases using Mn(IV) and Mn(III), Whelan[21] and Whelan and Sims[22] demonstrated that a set of equations, similar to Equations (2) through (6), can be developed for inner-sphere complex formation for Mn(III/IV) in both oxic and anoxic environments.

III. KINETICS OF REDUCTIVE DISSOLUTION AND AUTO-OXIDATION

The kinetics associated with reductive dissolution and auto-oxidation are reviewed for the surface interaction under oxic conditions of manganese(IV) dioxide and naphthalenediol, although the process is also applicable to the other constituents addressed herein. Assuming Equations (2) through (6) and Equation (8) are valid, the algorithms describing the kinetics of hypothetical reductive-dissolution and auto-oxidation reactions can be presented, as illustrated by Figure 3. By performing a theoretical surface mass balance, the total moles of surface sites per liter of solution (S_T) can be written as follows:

$$S_T = [\equiv Mn^{IV}(OH)_2] + [\equiv Mn^{IV}(O\text{-}Nap\text{-}OH)_2] + [\equiv Mn^{II}(\cdot O\text{-}Nap\text{-}OH)_2] + [\equiv Mn^{II}OH_2] + \qquad (10)$$

$[HO\text{-}(\equiv Mn^{IV})\text{-}OH_2]^+ + [HO\text{-}(\equiv Mn^{IV})\text{-}O]^- + [HO\text{-}Nap\text{-}O\text{-}(\equiv Mn^{IV})\text{-}O\text{-}Nap\text{-}OH_2]^+ +$

$[\equiv Mn^{IV}\text{-}(O\text{-}Nap\text{-}OH_2)_2]^{2+} + [HO\text{-}Nap\text{-}O\text{-}(\equiv Mn^{IV})\text{-}O\text{-}Nap\text{-}O]^- +$

$[\equiv Mn^{IV}\text{-}(O\text{-}Nap\text{-}O)_2]^{2-} + [\equiv Mn^{IV}\text{-}(OH_2)_2]^{2+} + [\equiv Mn^{IV}\text{-}O_2]^{2-}$

Assuming that the only species that contribute to the surface mass balance equation are $\equiv Mn^{IV}(OH)_2$, $\equiv Mn^{IV}(O\text{-}Nap\text{-}OH)_2$, $\equiv Mn^{II}OH_2$, and $\equiv Mn^{II}(\cdot O\text{-}Nap\text{-}OH)_2$, and that other competing anions and cations are not considered, the surface mass balance equation can be simplified as follows:

$$S_T = [\equiv Mn^{IV}(OH)_2] + [\equiv Mn^{IV}(O\text{-}Nap\text{-}OH)_2] + [\equiv Mn^{II}(\cdot O\text{-}Nap\text{-}OH)_2] + [\equiv Mn^{II}OH_2] \quad (11)$$

Under the assumption that each reaction can be described as an elementary reaction, rate expressions can be proposed for $\equiv Mn^{IV}(OH)_2$, $\equiv Mn^{IV}(O\text{-}Nap\text{-}OH)_2$, $\equiv Mn^{II}(\cdot O\text{-}Nap\text{-}OH)_2$, and $\equiv Mn^{II}OH_2$, using Equations (2) through (6) and Equation (11):

$$d[\equiv Mn^{IV}(OH)_2]/dt = - k_1 [Nap(OH)_2]^2 [\equiv Mn^{IV}(OH)_2] + k_4 [H^+]^2 [\equiv Mn^{II}OH_2] + k_{-1} [\equiv Mn^{IV}(O\text{-}Nap\text{-}OH)_2] \quad (12)$$

$$d[\equiv Mn^{IV}(O\text{-}Nap\text{-}OH)_2]/dt = k_1 [Nap(OH)_2]^2 [\equiv Mn^{IV}(OH)_2] - (k_{-1} + k_2) [\equiv Mn^{IV}(O\text{-}Nap\text{-}OH)_2] + k_{-2} [\equiv Mn^{II}(\cdot O\text{-}Nap\text{-}OH)_2] \quad (13)$$

$$d[\equiv Mn^{II}(\cdot O\text{-}Nap\text{-}OH)_2]/dt = k_2 [\equiv Mn^{IV}(O\text{-}Nap\text{-}OH)_2] - (k_{-2} + k_3) [\equiv Mn^{II}(\cdot O\text{-}Nap\text{-}OH)_2] + k_{-3} [\cdot O\text{-}Nap\text{-}OH]^2 [\equiv Mn^{II}OH_2] \quad (14)$$

$$d[\equiv Mn^{II}OH_2]/dt = k_3 [\equiv Mn^{II}(\cdot O\text{-}Nap\text{-}OH)_2] - (k_{-3} [\cdot O\text{-}Nap\text{-}OH]^2 + k_4 [H^+]^2) [\equiv Mn^{II}OH_2] \quad (15)$$

The rate expressions for the remaining nonsurface-constituent concentrations (i.e., $[Mn^{2+}]$, $[Nap(OH)_2]$, and $[\cdot O\text{-}Nap\text{-}OH]$) are as follows:

$$d[Mn^{2+}]/dt = k_4 [H^+]^2 [\equiv Mn^{II}OH_2] - k_5 [Mn_T] [P_{O_2}] [OH^-]^2 [Mn^{2+}] [Mn_T - Mn^{2+}] \quad (16)$$

$$d[Nap(OH)_2]/dt = - 2 k_1 [Nap(OH)_2]^2 [\equiv Mn^{IV}(OH)_2] + 2 k_{-1} [\equiv Mn^{IV}(O\text{-}Nap\text{-}OH)_2] \quad (17)$$

$$d[\cdot O\text{-}Nap\text{-}OH]/dt = 2 k_3 [\equiv Mn^{II}(\cdot O\text{-}Nap\text{-}OH)_2] - 2 k_{-3} [\cdot O\text{-}Nap\text{-}OH]^2 [\equiv Mn^{II}OH_2] \quad (18)$$

IV. RATE-LIMITING MECHANISM OF REDUCTIVE DISSOLUTION

Stone and Morgan[19] note that "(m)ost reductive dissolution reactions of environmental and geochemical significance are ... controlled by surface chemical reactions" and that transport-controlled reductive dissolution reactions represent rare cases. If either electron transfer [Equation (3)] or organic release [Equation (4)] represents the rate-limiting step for Mn(IV) in an oxic environment, Equations (3) through (6) can be represented by an overall reaction:

$$\equiv Mn^{IV}(O\text{-}Nap\text{-}OH)_2 \xrightarrow{k_6} Mn^{2+} + H_2O + \text{oxidized products} \qquad (19)$$

where k_6 is a rate constant in the forward direction. By performing a theoretical surface mass balance [see Equation (10)], assuming that the only species that contribute to the surface mass balance equation are $\equiv Mn^{IV}(OH)_2$ and $\equiv Mn^{IV}(O\text{-}Nap\text{-}OH)_2$, and that other competing anions and cations are not considered, the surface mass balance equation reduces to:

$$S_T = [\equiv Mn^{IV}(OH)_2] + [\equiv Mn^{IV}(O\text{-}Nap\text{-}OH)_2] \qquad (20)$$

The total manganese associated with the system (Mn_T) can be expressed as

$$Mn_T = [\equiv Mn^{IV}(OH)_2] + [\equiv Mn^{IV}(O\text{-}Nap\text{-}OH)_2] + Mn^{2+} \qquad (21)$$

By combining Equations (2), (19), and (21), assuming electron transfer/organic release represents the rate-limiting step (i.e., $d[\equiv Mn^{IV}(O\text{-}Nap\text{-}OH)_2]/dt$ is at steady state), and using a similar approach as that presented by Stone and Morgan[19], the rate of change in Mn^{2+} concentration can be determined as follows:[21]

$$\frac{d[Mn^{2+}]}{dt} = \frac{(k_6\,([Mn_T] - [Mn^{2+}]))\,[Nap\text{-}(OH)_2]^2}{((k_{-1} + k_6) / k_1) + [Nap\text{-}(OH)_2]^2} \qquad (22)$$

with the total number of remaining sites at time t being $[Mn_T] - [Mn^{2+}]$. The exponent on the organic substrate [i.e., molar ratio (R)] is two, representing the number of moles of organic oxidized to moles of Mn(IV) reduced [refer to

Equation (1)]. An expression similar to Equation (22), under oxic conditions, can also be developed for Mn(III) (e.g., MnOOH):[21,22]

$$\frac{d[Mn^{2+}]}{dt} = \frac{(k_6 ([Mn_T] - [Mn^{2+}])) [Nap\text{-}(OH)_2]}{((k_{-1} + k_6) / k_1) + [Nap\text{-}(OH)_2]} \quad (23)$$

The exponent on the organic substrate is unity [refer to Equation (14)]. Under the conditions of a mixture of Mn(III/IV) particles under nonhomogeneous conditions, an expression for the rate of change of Mn^{2+} can be calculated as[21,22]

$$\frac{d[Mn^{2+}]}{dt} = \sum_{i=1}^{m} \frac{k_{6i} ([Mn_T]_i - [Mn^{2+}]_i) [Nap\text{-}(OH)_2]^{Ri}}{((k_{-1i} + k_{6i}) / k_{1i}) + [Nap\text{-}(OH)_2]^{Ri}} \quad (24)$$

in which

$$[Mn_T] = \sum_{i=1}^{m} [Mn_T]_i \quad (25)$$

$$[Mn^{2+}] = \sum_{i=1}^{m} [Mn^{2+}]_i \quad (26)$$

where m is the number of different forms of manganese molecules (e.g., MnO_2, MnOOH, Mn_2O_3, δ-MnO_2, etc.) undergoing reductive dissolution, i is the index on the number of different forms of manganese molecules undergoing reductive dissolution, R is the ratio between the moles of organic oxidized to the moles of manganese reduced from Mn(IV/III) to Mn^{2+}, and all other terms retain their previous definition.

For Equation (22) to be qualitatively valid [and the more complex Equation (24)], the temporal change of 1) the organic substrate would have to have a shape similar to that exhibited by a rectangular hyperbola but decreasing with time and 2) Mn^{2+} would have to have a shape similar to a rectangular hyperbola that increases with time (i.e., as the manganese is reduced to Mn^{2+}, the substrate is oxidized). Many mathematical expressions describe a shape similar to a rectangu-

lar hyperbola over at least a portion of the region, including Michaelis-Menton, C $(1 - e^{-kt})$, etc. A relationship for the substrate that describes a shape similar to a rectangular hyperbola but decreasing with time is:[21,22]

$$[\text{Nap-(OH)}_2] = S_m K_s / (K_s + t) \quad (27)$$

where S_m and K_s are constants. Stone and Morgan[15] noted that for manganese the "initial dissolution rate is proportional to the amount of oxide loading, which suggests that the rate at any time during dissolution is proportional to the amount of remaining oxide ...." They described the initial dissolution rate with the following auto-catalytic expression:

$$d[Mn^{2+}]/dt = k_{exp} ([Mn_T] - [Mn^{2+}]) \quad (28)$$

where k_{exp} is the experimentally determined rate constant. Because Equation (28) is only applicable during the initial phases of reductive dissolution when the rate of change of Mn^{2+} production is proportional to the oxide solids remaining, it does not necessarily adequately describe the rate of dissolution over longer time periods. To account for auto-catalysis in the temporal rate of change of Mn^{2+} and the nonlinearity in this rate of change, Whelan[21] and Whelan and Sims[22] suggested a more appropriate expression for the time rate of change of Mn^{2+}:

$$d[Mn^{2+}]/dt = k_7 ([Mn_T] - [Mn^{2+}]) / (K_m + t)^2 \quad (29)$$

where k_7 and K_m are constants. During initial times, the temporal rate of change of Mn^{2+}, as expressed by Equation (29), exhibits linearity with the remaining oxide. During other phases of the process, Equation (29) also exhibits the nonlinearity inherent in the data. By integrating Equation (29), when $[Mn^{2+}]$ equals zero at time zero for the initial condition, a expression for Mn^{2+} as a function of time, can be developed:

$$[Mn^{2+}] = [Mn_T] \{1 - \exp [- k_7 t / K_m / (K_m + t)]\} \quad (30)$$

For Equation (30) to be valid, it should 1) have a shape similar to that exhibited by a rectangular hyperbola and 2) adequately describe the data. For example, 1) when time equals zero, $[Mn^{2+}]$ equals zero; 2) as time becomes large, the ratio of $[Mn^{2+}]/[Mn_T]$ approaches "1 - exp (k_7 / K_m)," not unity as a Michaelis-Menton-type rate expression would suggest; 3) Equation (30) has a shape similar to a rectangular hyperbola; and 4) the rate of change of Mn^{2+} is auto-catalytic [see Equation (29)]. By combining Equation (30) with Equation (27), the following expression can be derived:

$$\frac{d[Mn^{2+}]}{dt} = \frac{\{k_7 / (K_m - K_s)^2\} ([Mn_T] - [Mn^{2+}]) [Nap\text{-}(OH)_2]^2}{(K_s S_m)^2 + \{[Nap\text{-}(OH)_2] (K_m - K_s)\}^2 + 2 [Nap\text{-}(OH)_2] K_s S_m (K_m - K_s)} \quad (31)$$

By noting that $(K_s S_m) >> \{2 [Nap\text{-}(OH)_2] (K_m - K_s)\}$ should be valid over most of the range, Equation (31) reduces to a form that is the same as Equation (22):

$$\frac{d[Mn^{2+}]}{dt} = \frac{\{k_7 / (K_m - K_s)^2\} ([Mn_T] - [Mn^{2+}]) [Nap\text{-}(OH)_2]^2}{\{K_s S_m / (K_m - K_s)\}^2 + [Nap\text{-}(OH)_2]^2} \quad (32)$$

Utilizing the theoretical development leading to the derivation of Equation (32), manganese oxides were used to oxidize five multiple-ringed aromatic compounds containing diol and dione functional groups under oxic conditions in an aqueous environment: 1,4-, 1,3-, and 2,3-naphthalenediol, 1,4-naphthoquinone, and Quinizarin. The effectiveness of employing MnO_2 particles to oxidize these PAHs is best illustrated in the redox results presented in Figures 4 and 5. Figure 4 presents temporal variations in Mn^{2+} concentration by constituent, expressed as a fraction of the total manganese added to the reaction vessel. To indicate the degree of oxidation of the parent organics by the manganese particles, Figure 5 illustrates the fraction of the organic oxidized (i.e., molar ratio of organic oxidized to organic control) for 1,3- and 2,3-naphthalenediol and 1,4-naphthaquinone. For example, a 0.99 value in this figure indicates that

99% of the parent organic has been oxidized (either transformed or degraded); the possibility of sorption has been accounted for. Details of the experimental design and data are documented by Whelan.[21]

A nonlinear, least-squares regression analysis was performed on the data illustrated in Figure 4 using the SANREG statistical program.[37] The SANREG program uses the modified Gauss-Newton method for minimizing the sum-of-the-squares function. The results of this statistical analysis are also presented in Figure 4 and Table 1. Table 1 presents values for the coefficients k_7 and K_m for each of the organic chemicals. Point Day 4 in Figure 4 for the 1,4-naphthalenediol was not employed in the analysis as it is a significant outlier. Based on the data in Figures 4 and 5, Equations (29), (30), and (32) appear to describe the temporal variations in Mn^{2+} and the organic substrate as it relates to the reductive-dissolution process. These equations also satisfy the conditions for electron transfer/organic release as the rate-limiting step.

V. EFFECTS OF pH ON REDUCTIVE DISSOLUTION OF MANGANESE OXIDE PARTICLES

Equations (30) and (32) do not account for all relationships between reactants under varying environmental conditions (e.g., pH). Stone and Morgan[19], Whelan[21], and Whelan and Sims[22,28] have suggested that reductive dissolution of manganese oxides by organics is surface chemically controlled and not transport controlled. Therefore, assuming that electron transfer/release of aromatic organic is the rate-limiting step, Equations (3) through (6) can be condensed into the following expression:

$$\equiv Mn^{IV}(O\text{-}Nap\text{-}OH)_2 + n\ H^+ \xrightarrow{k_8} Mn^{2+} + H_2O + \text{oxidized products} \quad (33)$$

where k_8 is a rate constant in the forward direction, and n represents the number of moles of protons consumed in Equation (33). By combining Equations (2), (21),

and (33), and by using an approach similar to that presented by Stone and Morgan,[19] Whelan[21] derived the rate of change of Mn^{2+} as follows:

$$\frac{d[Mn^{2+}]}{dt} = \frac{k_8 ([Mn_T] - [Mn^{2+}]) (H^+)^n [Nap\text{-}(OH)_2]^2}{((k_{-1} + k_8 (H^+)^n) / k_1) + [Nap\text{-}(OH)_2]^2} \quad (34)$$

where (H^+) represents the proton activity with the total number of remaining sites at time t being $[Mn_T] - [Mn^{2+}]$. The organic term is squared because two moles of naphthalenediol are oxidized for each mole of manganese oxide reduced to Mn^{2+}.

Mathematically, Equation (34) describes the relationship between the rate of Mn^{2+} production, pH, and naphthalenediol concentration. If electron transfer/organic release is the rate limiting step, then $k_1 >> k_8$, and k_{-1} is most likely much larger than "$k_8 (H^+)^n$," thereby reducing Equation (34) to

$$\frac{d[Mn^{2+}]}{dt} = \frac{k_8 ([Mn_T] - [Mn^{2+}]) (H^+)^n [Nap\text{-}(OH)_2]^2}{(k_{-1} / k_1) + [Nap\text{-}(OH)_2]^2} \quad (35)$$

If $(k_{-1} / k_1) << [Nap\text{-}(OH)_2]^2$, which may be the case during the initial phases of the experiment when excess organic substrate is present, as illustrated by Stone and Morgan,[15] then Equation (35) reduces to

$$d[Mn^{2+}]/dt = k_8 ([Mn_T] - [Mn^{2+}]) (H^+)^n \quad (36)$$

Stone and Morgan[15] proposed an empirical equation for hydroquinone:

$$d[Mn^{2+}]/dt = k_9 ([Mn_T] - [Mn^{2+}]) (H^+)^m [QH_2] \quad (37)$$

where k_9 is a rate constant, m is a constant equaling 0.46, and QH_2 is hydroquinone. The power on QH_2 was determined to be unity; Stone and Morgan[15] mathematically demonstrated that the substrate hydroquinone is not squared because one mole of hydroquinone is oxidized for each mole of manganese dioxide reduced under anoxic conditions:

$$Mn^{IV}O_2(s) + QH_2 + 2\ H^+ = Mn^{2+} + Q + 2\ H_2O \quad (38)$$

where Q is benzoquinone. During the initial phases of the reductive dissolution process, Stone and Morgan[15] designed their experiments with hydroquinone in excess amounts; therefore, the hydroquinone concentration does not change significantly and can be considered in excess and a constant. As such, Equation (37) can be rewritten as follows:

$$d[Mn^{2+}]/dt = k_{10} ([Mn_T] - [Mn^{2+}]) (H^+)^m \quad (39)$$

in which

$$k_{10} = k_9 [QH_2] \quad (40)$$

where k_{10} is a rate constant. When the organic substrate is in excess, Equations (36) and (39) have the same form. A similar type of analysis can be employed when the remaining organic substrate has been nearly completely oxidized (i.e., $(k_{-1} / k_1) >> [Nap\text{-}(OH)_2]^2$); Equation (35) can be rewritten as follows:

$$d[Mn^{2+}]/dt = k_{11} ([Mn_T] - [Mn^{2+}]) (H^+)^n [Nap\text{-}(OH)_2]^2 \quad (41)$$

in which

$$k_{11} = (k_1 / k_{-1}) k_2 \quad (42)$$

where k_{11} is a rate constant. Equation (41) is very similar to Equation (37).

Stone[26] performed a similar analysis using phenol when determining the exponent on the proton concentration by solving the following equation:

$$d[Mn^{2+}]/dt = k_{12} (H^+)^q [phenol]^p \quad (43)$$

where k_{12} is a rate constant and p and q are exponents. He solved for q and found that it ranged from <0.5 when pH of 4 was approached to greater than unity for pHs greater than 6. Equation (43) is very similar in form to Equation (41).

Equation (33) describes the functional role that protons play in the reductive-dissolution process during the oxidation of aromatics. Protons are consumed in this process, and a decrease in the pH should increase the reductive-dissolution rate. Figures 6 and 7 present the effects that variations in pH have on the

reduction dissolution of Mn(III/IV) to dissolved Mn(II) and oxidation of 2,3-naphthalenediol, respectively. These figures present the results of three different initial pH levels with all other conditions being equal: 4.58, 5.85, and 8.75.

Figure 6 presents the temporal variation in the dissolved manganese concentration by initial pH, expressed as a fraction of the total manganese added to the reaction vessel. Correspondingly, to indicate the degree of oxidation of the parent organics by the manganese particles, Figure 7 presents the fraction of the organic oxidized (i.e., molar ratio of organic oxidized to organic control). The results presented in Figures 6 and 7 complement each other and appear to follow the shapes suggested by Equation (34). Details of the experimental design and data are documented by Whelan.[21]

A nonlinear, least-squares regression analysis was performed on the data illustrated in Figure 6 using the SANREG statistical program[37] and assuming the validity of Equations (29), (30), (34), (35), and (41). The results of this statistical analysis are also presented in Figure 6 and Table 2. Table 2 presents values for the coefficients k_7 and K_m for Day 14 under varying pH conditions. In addition, the final pH of each solution, based on separate triplicate sampling tubes, is also presented.

An analysis was performed to estimate the exponent "n" on the proton concentration in Equation (41). The condition associated with Equation (41) is chosen (i.e., $(k_{-1} / k_1) >> [Nap\text{-}(OH)_2]^2$), as opposed to that associated with Equation (36) (i.e., $(k_{-1} / k_1) << [Nap\text{-}(OH)_2]^2$), because most of the dissolved Mn(II) and naphthalenediol data collected represent long-term information (i.e., on the order of weeks) (see Figures 6 and 7). If Equation (36) were employed, short-term

data (i.e., on the order of minutes) would have to have been collected. By combining Equations (29) and (41), the following expression can be derived

$$\frac{d[Mn^{2+}]}{dt} = \frac{k_7 ([Mn_{T1} - [Mn^{2+}])}{(K_m + t)^2} = k_5 ([Mn_T] - [Mn^{2+}]) [Nap\text{-}(OH)_2]^2 (H^+)^n \quad (44)$$

Linearizing Equation (44) gives

$$Log (RATIO) = Log (k_5 [Nap\text{-}(OH)_2]^2) - n\ pH \quad (45)$$

in which

$$RATIO = k_7 / (K_m + t)^2 \quad (46)$$

Day 14 results of Equation (45) are plotted in Figure 8 with a correlation coefficient (r^2) of 96%. The negative slope of the curve represents the exponent "n" and has a value of 0.4, which is similar to the value of 0.46 that Stone and Morgan[15] found for the oxidation of hydroquinone using reductive dissolution.

VI. POLYMERIC PRODUCTS OF NAPHTHALENEDIOL FROM REDUCTIVE DISSOLUTION

Figure 3 and Equations (4), (19), and (33) suggest that if a free radical represented an intermediate step, one potential product of abiotic-catalyzed, reductive dissolution was an oxidized or "humified" polymer. The precipitate had a deep, dark-brown color, similar to that exhibited by humic polymers. The redox reaction between MnO_2 particles and naphthalenediol resulted in the formation of such a precipitate. It was insoluble in dichloromethane, acetonitrile, and water at various pHs. Three analyses were performed to determine the origin of the material: infrared (IR) spectroscopy; microelemental determination for carbon, oxygen, and hydrogen; and scanning electron microscopy using an energy-dispersive x-ray analysis (EDXA).

The results of the IR are presented in Figure 9. Even though the sample had been dried in a 103°C oven for 24 hours, the material was so hydroscopic that

water was still abundant in the spectral curve. Figure 9 presents percent transmission versus frequency in wave numbers over a range of 3600 to 600 cm^{-1}. Various bands occur near 3440, 2924, 2855, 1622, 1456, 1384, 1289, and 1234 cm^{-1}, and at other bands in the fingerprint region (i.e., <1400 cm^{-1}). Based on previous analyses by Stevenson,[6] this spectral curve appears to correspond to an organic compound similar in nature to that of a polymerized naphthalenediol product.[21,28]

The distribution of carbon, oxygen, and hydrogen by weight in naphthalenediol is 75.0%, 20.0%, and 5.0%, respectively. A microelemental analysis determined the composition based on weight of the organic residue as 63.7%, 25.2%, and 4.2% of carbon, oxygen, and hydrogen, respectively, thereby accounting for 93.1%; 6.9% is unaccounted for. Illustrative results of the EDXA are presented in Figure 10 and were used to identify the remaining 6.9% as that of Cl^-. Chloride was the only "element" that appeared in residue samples but did not appear in background samples. The percentages by weight of the chloride in particle samples ranged from 2.5% to 8.0%. The chloride originates from the $NaClO_4$, which was used to fix the ionic strength of each solution. At a concentration of 10^{-3} M, $NaClO_4$ can supply plenty of available chloride. The 5.2% oxygen in excess of that present in the naphthalenediol (i.e., 20.0% versus 25.2%) can also be attributed to the perchlorate ion (ClO_4^-).

VII. SUMMARY

The research outlined in this manuscript involves one dominant theme: Can manganese reductive dissolution oxidize multiple-ringed aromatic compounds in an oxic environment, keeping in mind that recalcitrant PAH compounds are of ultimate interest? This research indicated that certain forms of PAH compounds (e.g., dihydrodiols and diones that form free-radical intermediates) are susceptible to

oxidation and polymerization. For example, all aromatic compounds exhibited varying degrees of oxidation over a 14-day period, resulting in 83%, 76%, 54%, 70%, and 20% of the manganese being reduced by 2,3-, 1,3-, and 1,4-naphthalenediol, Quinizarin, and 1,4-naphthoquinone, respectively. Correspondingly, after 14 days, 100% of the 2,3- and 1,3-naphthalenediol was oxidized, while approximately 65% of the 1,4-naphthalenediol was oxidized. Aromatics with diol functional groups were more successful at reducing manganese (and, hence, being oxidized) than those with only dione functional groups. The results also demonstrated that relatively insoluble aromatic compounds like Quinizarin can be oxidized. The oxidation of Quinizarin resulted in a significant reduction of manganese particles from Mn(IV) to Mn(II) (i.e., 70%) over a 14-day period. Insoluble "humic-like" material precipitated during the reactions, indicating that a polymerization/humification process was occurring. Finally, the results suggested that electron transfer/organic release from the oxide surface is the rate-limiting step.

Acknowledgments-Funding for this research was supplied by the U.S. Geological Survey through a grant to Utah State University (USU) under Award No. 14-08-0001-G1723. Thanks are extended to Drs. J. J. Jurinak and D. K. Stevens of USU, J.-M. Bollag of Pennsylvania State University, A. T. Stone and K. L. Godfredtsen of Johns Hopkins University, and P. M. Huang of the University of Saskatchewan for providing technical information during the various phases of this work. Thanks are also extended to Dr. S. V. Mattigod of Battelle, Pacific Northwest Laboratories (BNW) for his technical review and comments. Appreciation is extend to Ms. J. Gephart and Mr. J. Flynn of BNW, and BNW for performing the editorial review of and providing funding for this manuscript, respectively.

VIII. REFERENCES

1. Bollag, J.-M., and Liu, S.-Y., Biological transformation processes of pesticides, in *Pesticides in the Soil Environment*, Cheng, H.H. Ed., Soil Science Society of America, Madison, Wisconsin, 1990, chap. 6.
2. Sarkar, J. M., Malcolm, R. L., and Bollag, J.-M., Enzymatic coupling of 2,4-dichlorophenol to stream fulvic acid in the presence of oxidoreductases, *Soil Sci. Soc. Amer. J.*, 52, 688, 1988.
3. Martin, J. P., Haider, K., and Linhares, L. F., Decomposition and stabilization of ring ^{14}C-labelled catechol in soil, *Soil Sci. Soc. Am. J.*, 43, 100, 1979.
4. Liu, S.-Y., Freyer, A. J., Minard, R. D., and Bollag, J.-M., Enzyme-Catalyzed complex formation of amino acid esters and phenolic humus constituents, *Soil Sci. Soc. Amer. J.*, 49, 337, 1985.
5. Bollag, J.-M. and Myers, C., Detoxification of aquatic and terrestrial sites through binding of pollutants to humic substances, *Sci. Tot. Environ.*, in press.
6. Stevenson, F. J., *Humus Chemistry: Genesis Composition, Reactions*, John Wiley & Sons, New York, 1983.
7. Wang, M. C. and Huang, P. M., Catalytic power of nontronite, kaolinite and quartz and their reaction sites in the formation of hydroquinone-derived polymers, *Appl. Clay Sci.*, 4, 43, 1989.
8. Haider, K., Martin, J. P., and Filip, Z., Humus biochemistry, in *Soil Biochemistry*, Vol. 4, Paul, E.A. and McLanen, A.D. Eds., Marcel Dekker, New York, 1975, 195.
9. Flaig, W., Beutelspacher, H., and Rietz, E., Chemical composition and physical properties of humic substances, in *Soil Components, Vol. 1, Organic*

Components, Gieseking, J. E. Ed., Springer-Verlag, New York, 1975, 1.

10. Shindo, H. and Huang, P. M., Catalytic effects of manganese(IV), iron(III), aluminum, and silicon oxides on the formation of phenolic polymers, *Soil Sci. Soc. Amer. J.*, 48, 927, 1984.

11. Whelan, G. and Sims, R. C., Abiotic immobilization/detoxification of recalcitrant organics, in *Proc. of SUPERFUND '90*, Hazardous Materials Control Research Institute, Silver Spring, Maryland, 1990, 820.

12. Qiu, X. and McFarland, M. J., Bound residue formation in PAH contaminated soil composting using *Phanerochaete chrysosporium*, *Haz. Waste and Haz. Mat.*, 8, 115, 1991.

13. Abbott, C. A. and Sims, R. C., Use and efficiency of ethylene glycol monomethyl ether and monoethanolamine to trap volatilized [7-^{14}C] naphthalene and ^{14}C carbon dioxide, in *Proc. of SUPERFUND '89*, Hazardous Materials Control Research Institute, Silver Spring, Maryland, 1989, 23.

14. Laha, S. and Luthy, R. G., Oxidation of aniline and other primary aromatic amines by manganese dioxide, *Environ. Sci. Technol.*, 24, 363, 1990.

15. Stone, A. T. and Morgan, J. J., Reduction and dissolution of manganese(III) and manganese(IV) oxides by organics. 1. Reaction with hydroquinone, *Environ. Sci. Technol.*, 18, 450, 1984.

16. Stone, A. T. and Morgan, J. J., Reduction and dissolution of manganese(III) and manganese(IV) oxides by organics. 2. Survey of the reactivity of organics, *Environ. Sci. Technol.*, 18, 617, 1984.

17. Mihelcic, J. R. and Luthy, R. G., Degradation of polycyclic aromatic hydrocarbon compounds under various redox conditions in soil-water systems, *Appl. Environ. Microbiol.*, 54, 1182, 1988.

18. **Musso, H.**, Phenol coupling, in *Oxidative Coupling of Phenols*, Taylor, W. I. and Battersby, A. R. Eds., Marcel Dekker, New York, 1967, 1.

19. **Stone, A. T. and Morgan, J. J.**, Reductive dissolution of metal oxides, in *Aquatic Surface Chemistry*, W. Stumm Ed., John Wiley & Sons, New York, 1987, 221.

20. **Whelan, G. and Sims, R. C.**, Oxidation of recalcitrant organics in subsurface systems, *Haz. Waste Haz. Mat.*, in press.

21. **Whelan, G.**, Surface-Induced oxidation of multiple-ringed diol and dione aromatics by manganese dioxide, Ph.D. Dissertation, Utah State University, Logan, Utah, 1992.

22. **Whelan, G. and Sims, R. C.**, Abiotic-Catalyzed oxidation of naphthalenediol, naphthoquinone, and dihydroxyanthracenedione, *Environ. Sci. Technol.*, in review.

23. **Shindo, H. and Huang, P. M.**, Role of manganese(IV) oxide in abiotic formation of humic substances in the environment, *Nature* (London), 298, 363, 1982.

24. **LaKind, J. S. and Stone, A. T.**, Reductive dissolution of geothite by phenolic reductants, *Geochim. Cosmochim. Acta*, 53, 961, 1989.

25. **Shindo, H. and Huang, P. M.**, Catalytic polymerization of hydroquinone by primary minerals, *Soil Sci.*, 139, 505, 1985.

26. **Stone, A. T.**, Reductive dissolution of manganese(III/IV) oxides by substituted phenols, *Environ. Sci. Technol.*, 21, 979, 1987.

27. **Taylor, W. I. and Battersby, A. R.**, Eds., *Oxidative Coupling of Phenols*, Marcel Dekker, New York, 1967, vii.

28. **Whelan, G. and Sims, R. C.**, Abiotic-Catalyzed Oxidation of 2,3-Naphthalenediol, *Environ. Toxicol. Chem.*, in review.

29. **Stone, A. T. and Ulrich, H.-J.**, Kinetics and reaction stoichiometry in the reductive dissolution of manganese(IV) dioxide and Co(III) oxide by hydroquinone, *J. Colloid. Inter. Sci.*, 132, 509, 1989.

30. **Furrer, G. and Stumm, W.**, The coordination chemistry of weathering: I. Dissolution kinetics of δ-Al_2O_3 and BeO, *Geochim. Cosmichim. Acta*, 50, 1847, 1986.

31. **Stumm, W. and Morgan, J. J.**, *Aquatic Chemistry*, 2nd Ed., John Wiley & Sons, New York, 1981.

32. **Benefield, L. D., Judkins, J. F., and Weand, B. L.**, *Process Chemistry for Water and Wastewater Treatment*, Prentice-Hall, New York, 1982.

33. **Morgan, J. J.**, Chemical equilibria and kinetic properties of manganese in natural waters, in *Principles and Applications of Water Chemistry*, Faust, S. D. and J. V. Hunter Eds., John Wiley & Sons, New York, 1967, 561.

34. **Wehrli, B.**, Redox Reactions of Metal Ions at Mineral Surfaces, in *Aquatic Chemical Kinetics: Reaction Rates of Processes in Natural Waters*, W. Stumm Ed., John Wiley & Sons, New York, 1990, 311.

35. **Diem, D. and Stumm, W.**, Is dissolved Mn^{2+} being oxidized by O_2 in absence of Mn-Bacteria or surface catalysts?, *Geochim. Cosmochim. Acta*, 48, 1571, 1984.

36. **Wilson, D. E.**, Surface and complexation effects on the rate of Mn(II) oxidation in natural waters, *Geochim. Cosmochim. Acta*, 44, 1311, 1980.

37. **Stevens, D. K.**, SANREG statistical computer program, unpublished, Department of Civil and Environmental Engineering, Utah State University, Logan, Utah, 1992.

TABLE 1 Values for Coefficients Associated with the Rectangular-Hyperbola Curve Describing the Temporal Variation of Mn^{2+} Concentration, Based on a Nonlinear, Least-Squares Regression Analysis of Five, Multiple-Ringed, Aromatic Chemicals[21]

Chemical	k_7 (day)	K_m (day)
1,4-Naphthalenediol	0.18	0.23
2,3-Naphthalenediol	1.50	0.86
1,3-Naphthalenediol	0.29	0.20
1,4-Naphthoquinone	406.	156.
Quinizarin	1.87	1.45

Table 2. Values for Coefficients Associated with the Rectangular-Hyperbola Curve Describing the Temporal Variation of Mn^{2+} Concentration, Based on a Nonlinear, Least-Squares Regression Analysis for 2,3-Naphthalenediol Under Varying pH Conditions at Day 14[21]

pH		k_7	K_m
Initial	Final	(day)	(day)
4.58	5.51 ± 1.00	1.50	0.86
5.85	6.10 ± 1.16[(a)]	0.79	1.24
8.75	6.99 ± 0.30	0.46	1.12

[(a)]Based on Day 7.

FIGURE CAPTIONS

Figure 1. Proposed relationships between naphthalenediol, semiquinone radical, naphthoquinone, semiquinone radical anion, and semiquinone dianion[19-22]

Figure 2. Schematic Diagram of 1,4-, 2,3-, 1,3-Naphthalenediol, 1,4-Naphthoquinone, and 1,4-Dihydroxy-9,10-Anthracenedione[21,22]

Figure 3. Schematic of the reductive-dissolution/auto-oxidation process[19-22]

Figure 4. Nonlinear, least-squares regression plots associated with the fraction of the total manganese as dissolved Mn^{2+} in a buffered system[21,22]

Figure 5. Fraction of the organic substrate oxidized during reductive dissolution[21,22]

Figure 6. Nonlinear, least-squares regression plots associated with the fraction of total manganese as dissolved Mn^{2+} as a function of initial pH with 2,3-naphthalenediol[21,22]

Figure 7. Temporally varying fraction of 2,3-naphthalenediol oxidized during reductive dissolution as a function of pH[21,28]

Figure 8. Log(RATIO) versus pH[21,28]

Figure 9. Infrared spectroscopy of naphthalenediol residue[21,28]

Figure 10. Energy-Dispersive x-ray analysis of precipitate residue[21,28]

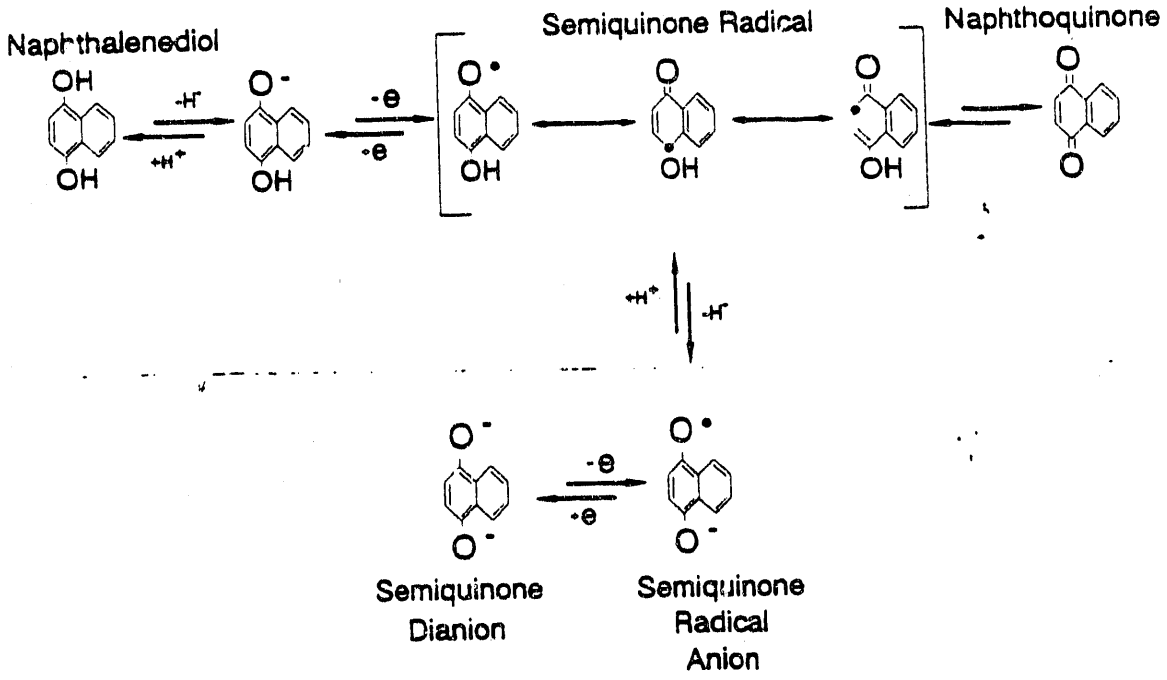
Naphthalenediol
Semiquinone Radical
Naphthoquinone
OH
OH
-H+
+H+
O-
OH
-e
+e
O•
OH
O
OH
O
O
+H+
-H+
O-
O-
-e
+e
O•
O-
Semiquinone Dianion
Semiquinone Radical Anion

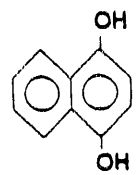

1,4-Naphthalenediol

2,3-Naphthalenediol

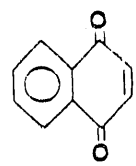

1,4-Naphthoquinone

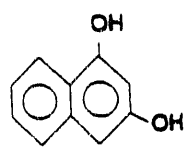

1,3-Naphthalenediol

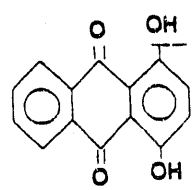

1,4-Dihydroxy-9,10-anthracenedione
(Quinizarin)

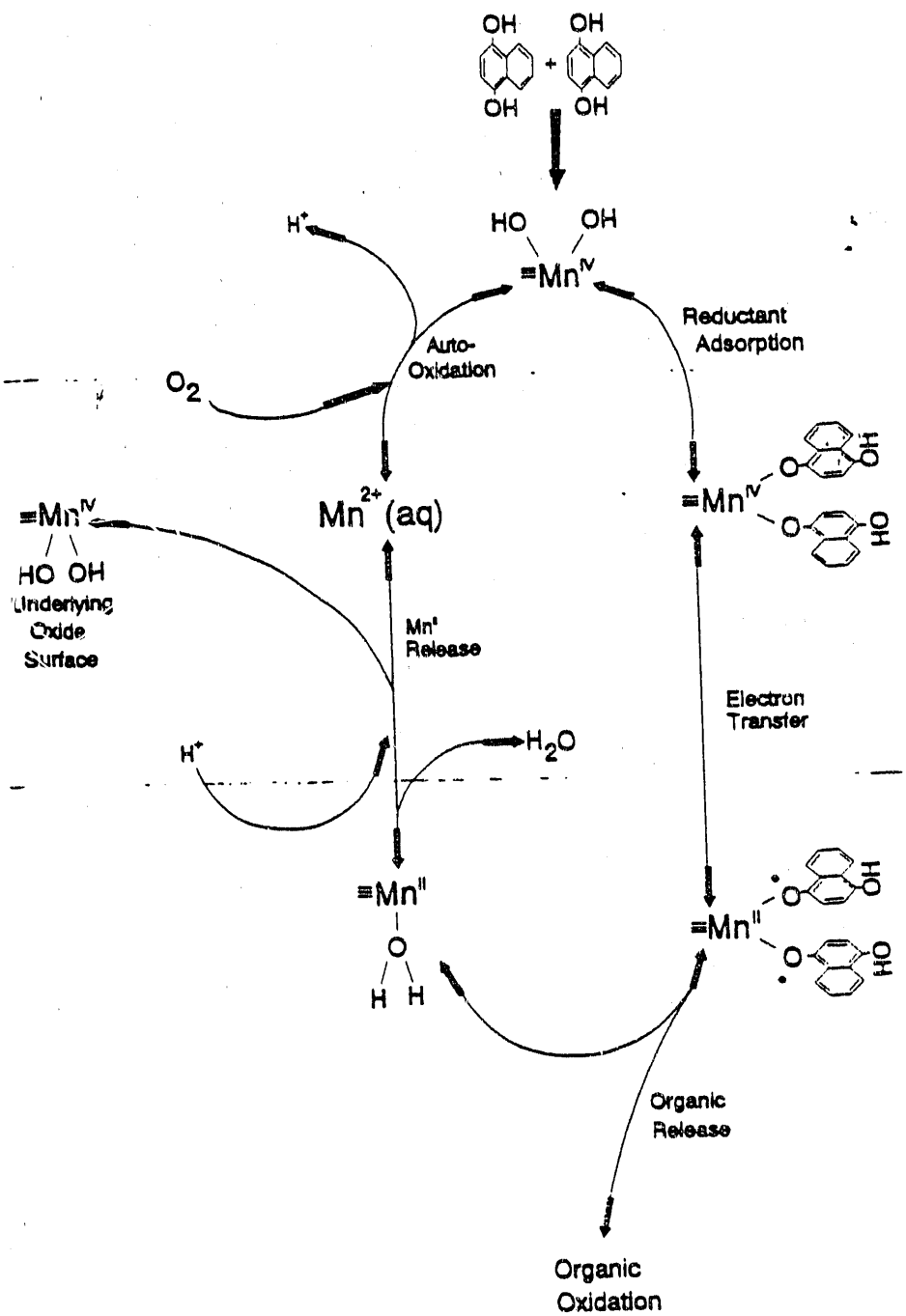
OH
OH
OH
OH
H+
HO
OH
≡Mn^IV
Reductant
Adsorption
Auto-
Oxidation
O2
Mn^2+ (aq)
≡Mn^IV
HO OH
Underlying
Oxide
Surface
Mn^II
Release
Electron
Transfer
H+
H2O
≡Mn^II
O
H H
≡Mn^II
Organic
Release
Organic
Oxidation

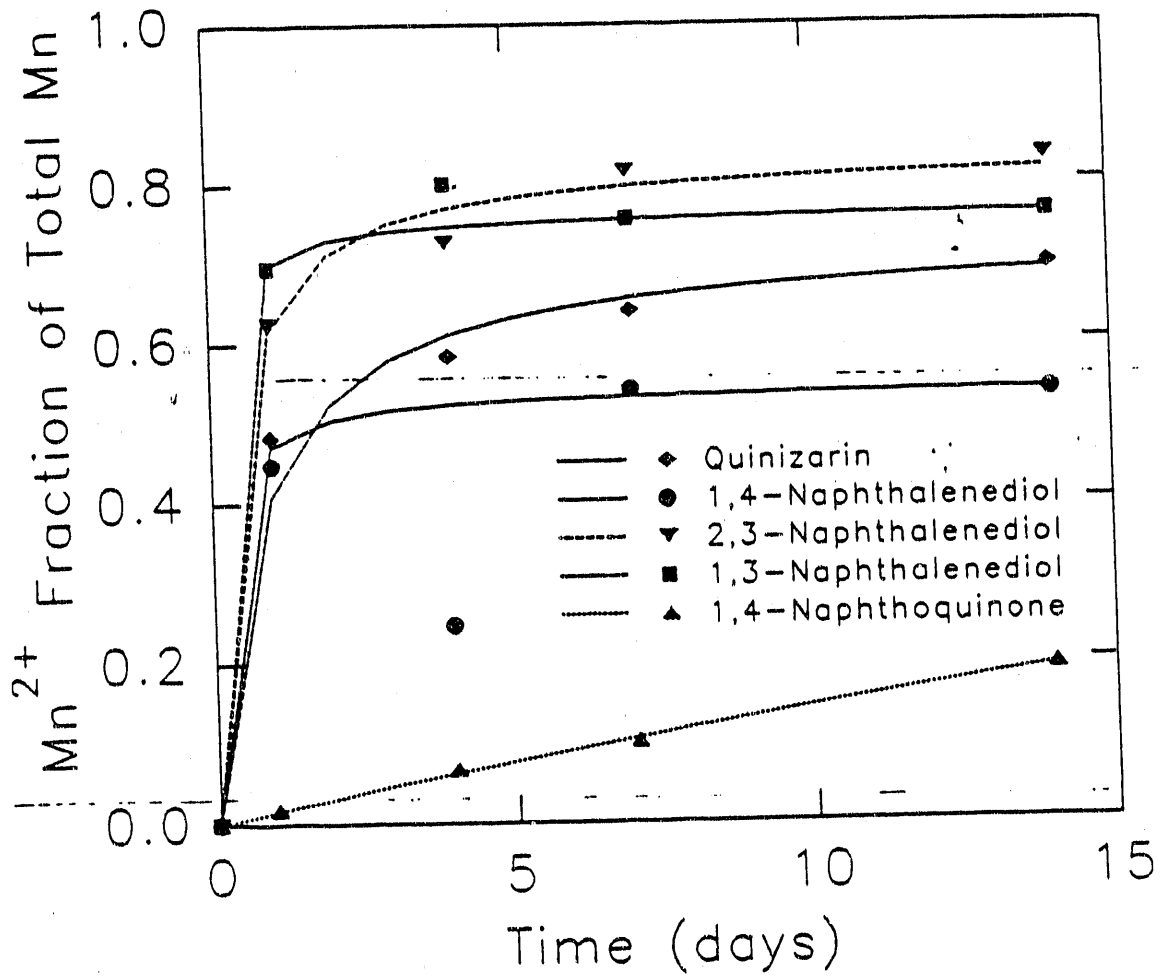
1.0
0.8
0.6
0.4
0.2
0.0
Mn^{2+} Fraction of Total Mn
0
5
10
15
Time (days)
Quinizarin
1,4-Naphthalenediol
2,3-Naphthalenediol
1,3-Naphthalenediol
1,4-Naphthoquinone

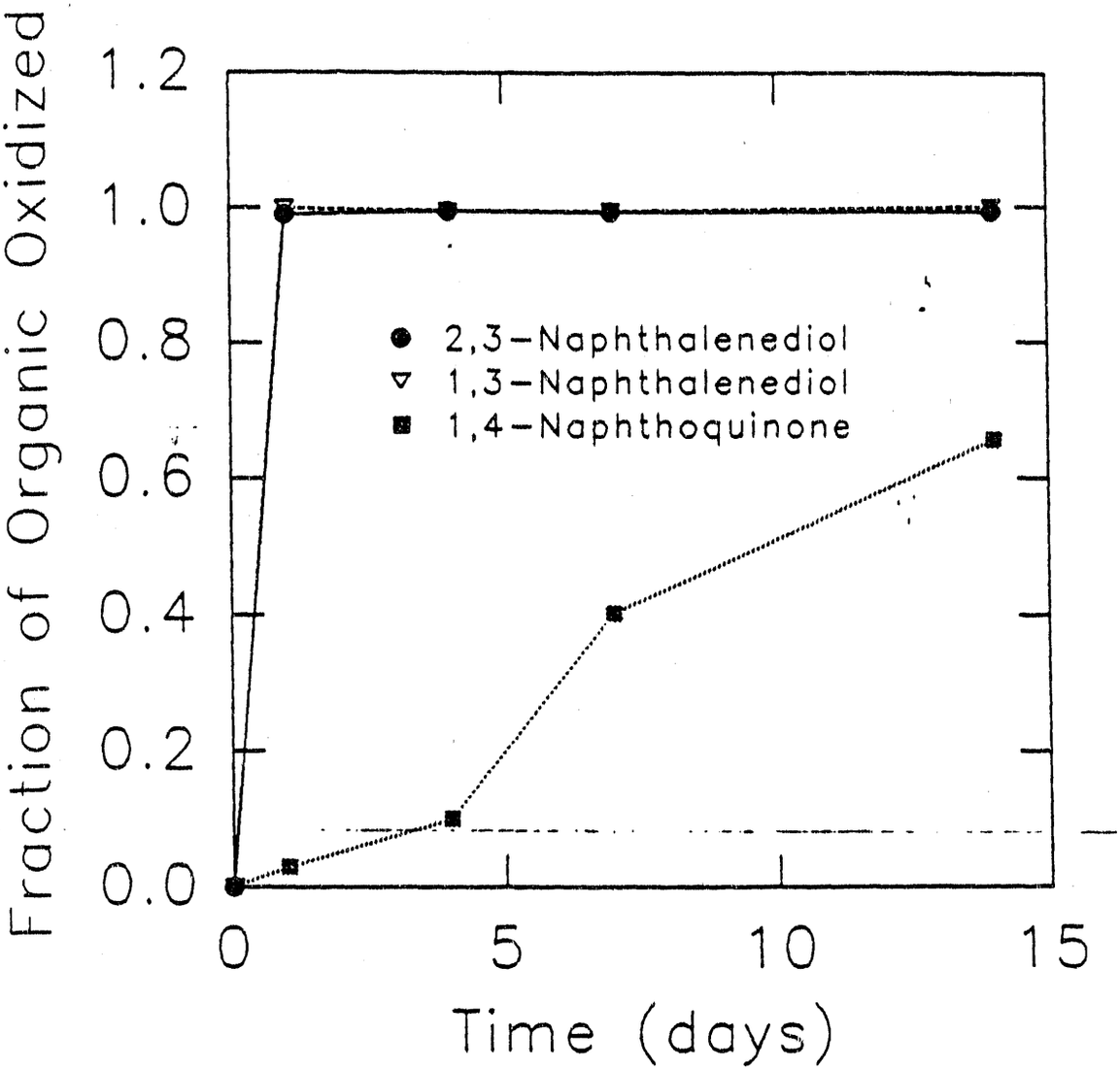
Fraction of Organic Oxidized
1.2
1.0
0.8
0.6
0.4
0.2
0.0
0
5
10
15
Time (days)
2,3-Naphthalenediol
1,3-Naphthalenediol
1,4-Naphthoquinone

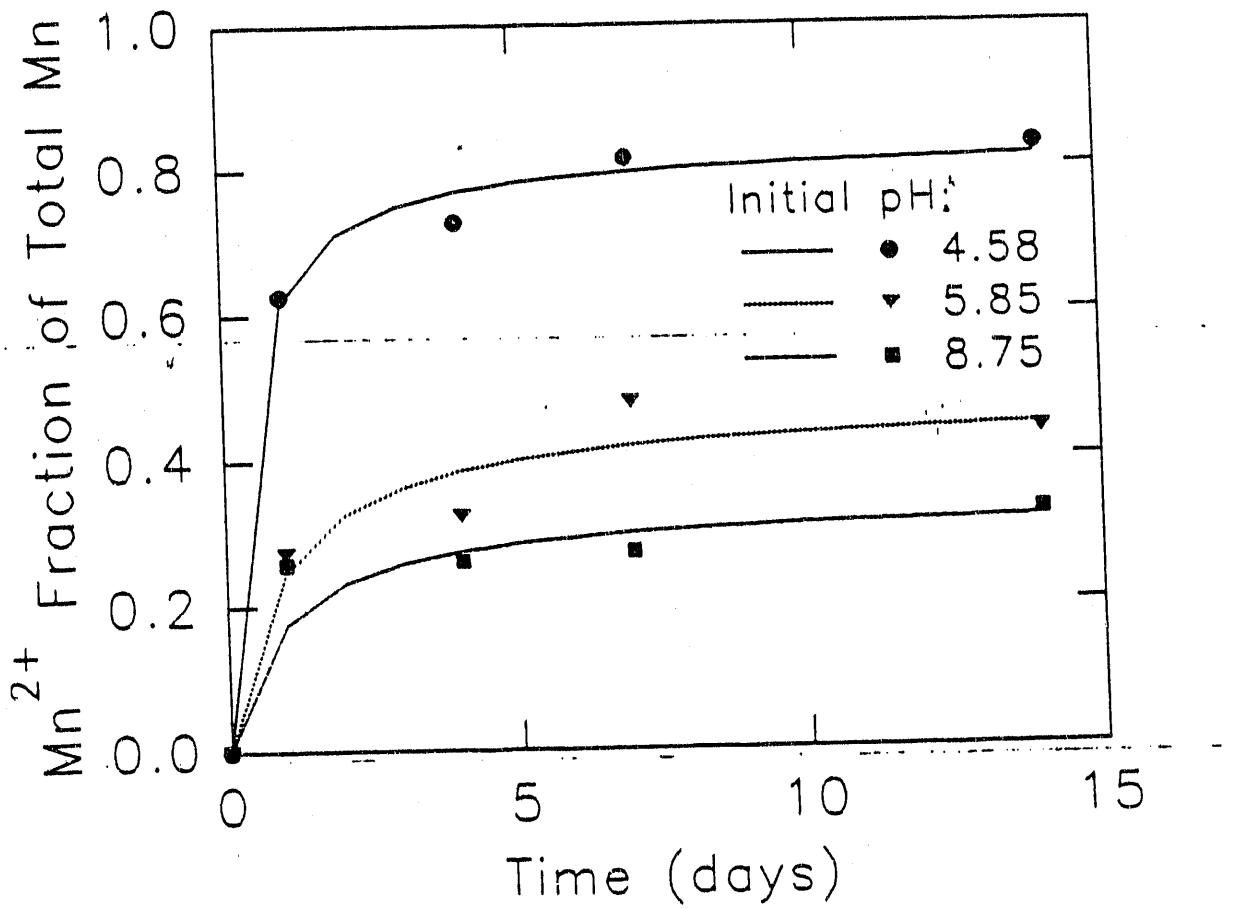
1.0
0.8
0.6
0.4
0.2
0.0
Mn2+ Fraction of Total Mn
0
5
10
15
Time (days)
Initial pH:
4.58
5.85
8.75

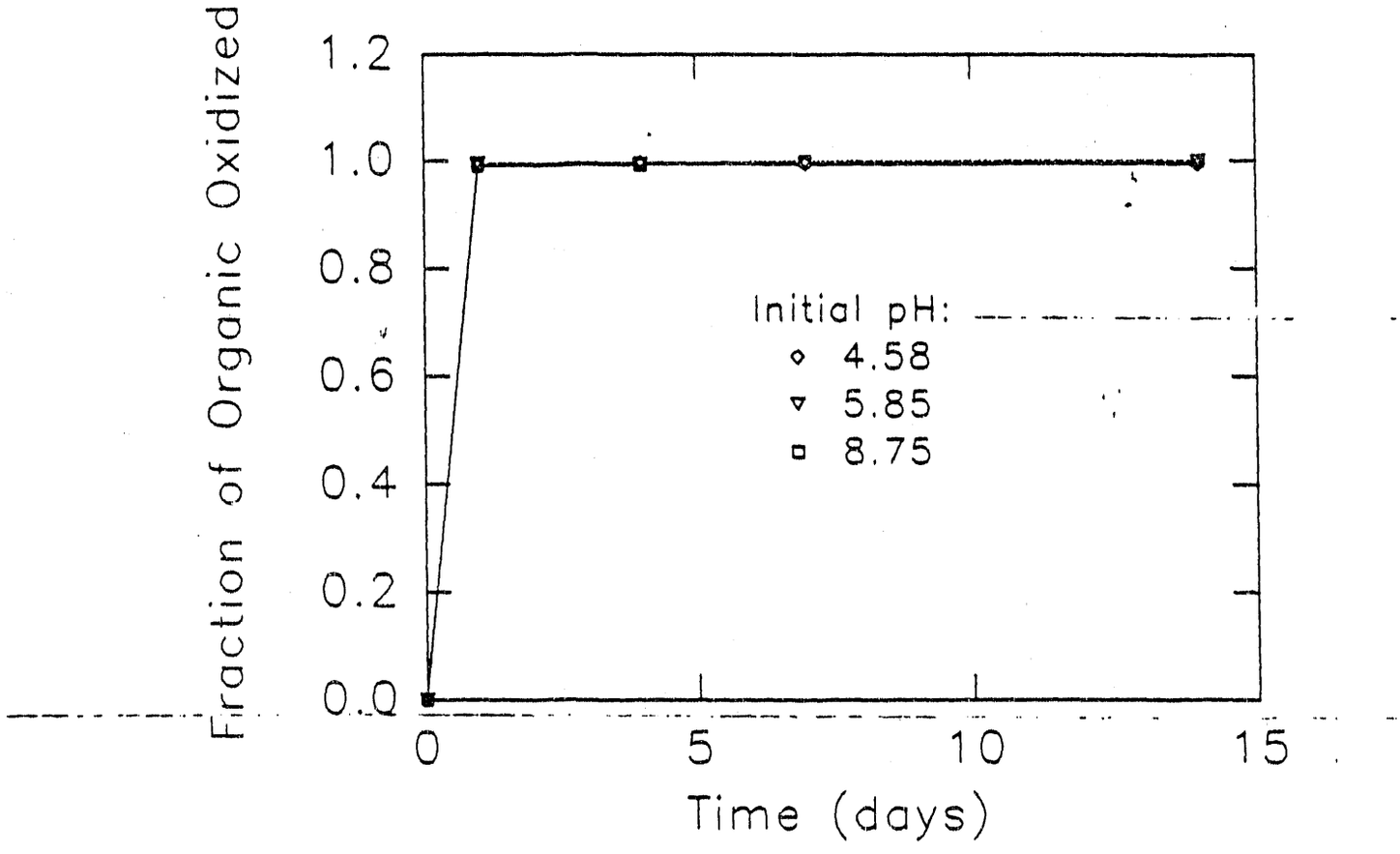
Fraction of Organic Oxidized
1.2
1.0
0.8
0.6
0.4
0.2
0.0
0
5
10
15
Time (days)
Initial pH:
4.58
5.85
8.75

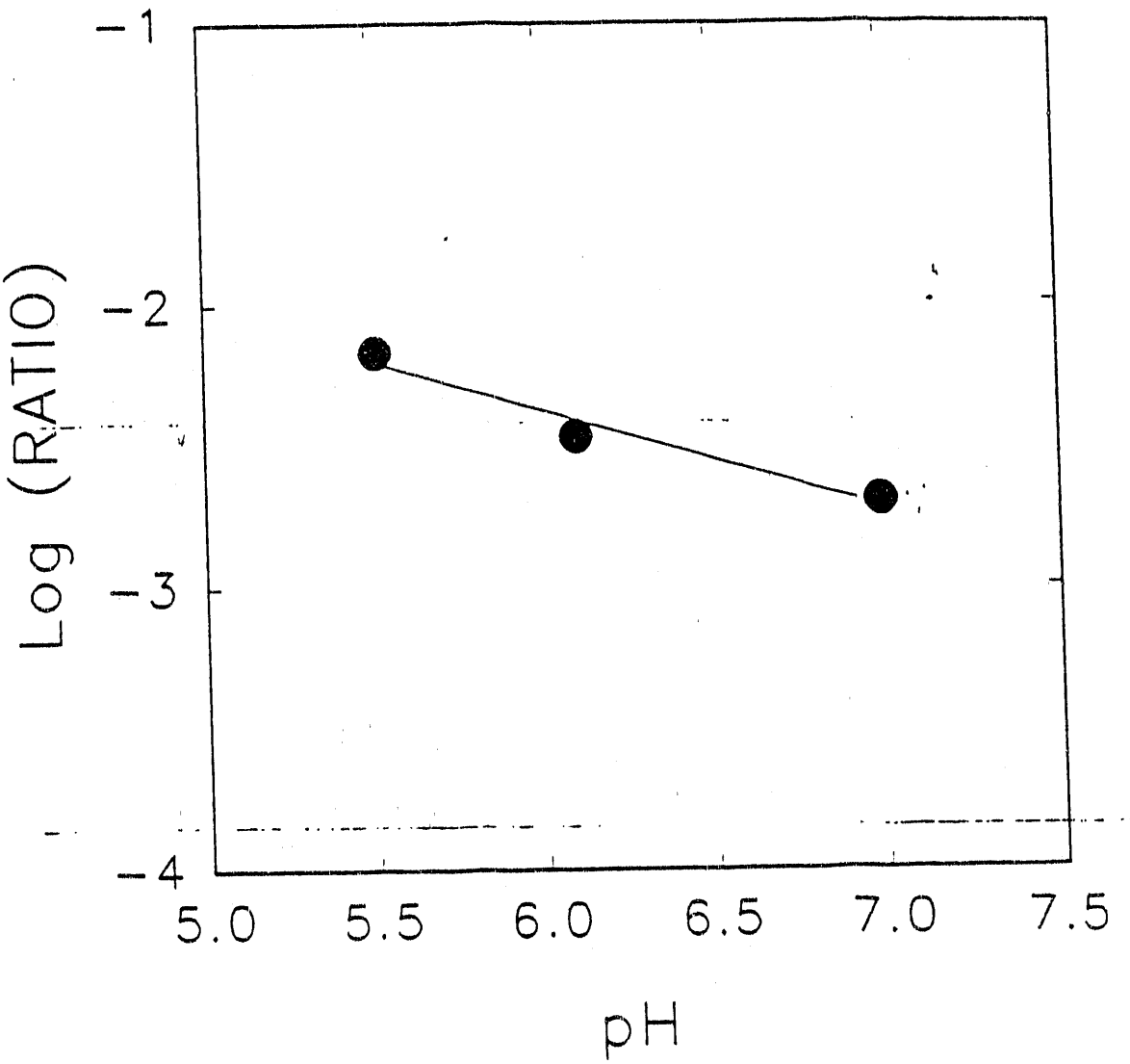
-1
-2
-3
-4
Log (RATIO)
5.0
5.5
6.0
6.5
7.0
7.5
pH

END

DATE FILMED

12 / 17 / 92